Available online at www.sciencedirect.com
SCIENCE DIRECT®
Journal of Power Sources 119–121 (2003) 285–289
JOURNAL OF POWER SOURCES
www.elsevier.com/locate/jpowsour

A new type of orthorhombic $LiFeO_2$ with advanced battery performance and its structural change during cycling

Y.S. Lee[a], S. Sato[b], Y.K. Sun[c], K. Kobayakawa[b], Y. Sato[b,*]

[a]*High-Tech Research Center, Kanagawa University, 3-27-1 Rokkakubashi, Yokohama 221-8686, Japan*
[b]*Department of Applied Chemistry, Kanagawa University, 3-27-1 Rokkakubashi, Yokohama 221-8686, Japan*
[c]*Department of Chemical Engineering, Hanyang University, 17 Haengdang-dong, Seoul 133-791, South Korea*

Abstract

Nano-crystalline $LiFeO_2$ has been synthesized at low temperature (150 °C) using the solid-state method. It was composed of orthorhombic $LiFeO_2$ and a small amount of spinel $LiFe_5O_8$ phases. A Li/$LiFeO_2$ cell showed not only a fairly high initial discharge capacity of over 150 mAh/g, but also a good cycle retention rate at room temperature. We first found that the orthorhombic $LiFeO_2$ underwent a structural change to the spinel phase ($LiFe_5O_8$) during the charge/discharge process, which resulted in the capacity decline of the Li/$LiFeO_2$ system.

Keywords: Nano-crystalline; Orthorhombic $LiFeO_2$; Cycleability; $LiFe_5O_8$; Phase change

1. Introduction

The battery industries have aimed to supply safe power sources with high energy density and good cycle performance. Lithium secondary batteries are the most promising candidate among the many possibilities to satisfy this demand. Many research groups have investigated various cathode materials for the lithium secondary batteries such as layered oxides; $LiMO_2$ (M: Co, Ni, Mn, Fe, ...) [1–6]. Layered lithium metal oxide has a rock salt structure where lithium and a transition metal cation occupy alternate layers of octahedral sites in a distorted close-packed oxygen ion lattice.

$LiCoO_2$ has many problems such as high cost, environmental concerns, and low practical capacity (about 130 mAh/g) [1,2]. Although $LiNiO_2$ has a higher practical capacity than $LiCoO_2$, it is highly possible that exothermic decomposition of the oxide will occur by releasing oxygen at high temperature [3,4]. $LiMnO_2$ still shows a small discharge capacity in the 4 V region, which is a problem for it's commercialization, especially the orthorhombic type, because of the increasing initial discharge capacity in the early stage [5,6].

$LiFeO_2$ has many advantages over these layered cathode materials because it is nontoxic and contains the most abundant metal in the world. It is well known that $LiFeO_2$ has different forms, i.e. the α-, β-, and γ-forms, due to the synthetic conditions and synthetic method. The α-$LiFeO_2$ is a cubic unit cell of space group *Fm*3*m*, β-$LiFeO_2$ (monoclinic, *C*2/*c*) is formed by an intermediate phase during the ordering process. The γ-$LiFeO_2$ (tetragonal, $I4_1/amd$) is obtained by reducing the symmetry from cubic to tetragonal by ordering the Li^+ and Fe^{3+} ions at octahedral sites [7–15].

Kanno and coworkers [7,8], found that the corrugated layered structure $LiFeO_2$ compound was electrochemically active during the lithium insertion/extraction reaction. They succeeded in synthesizing $LiFeO_2$ from γ-FeOOH using the H^+/Li^+ ion exchange reaction at a reaction temperature of 100–500 °C. Although this Li/$LiFeO_2$ cell exhibited a fairly high initial discharge capacity of about 100 mAh/g and lithium reversibly inserts/extracts in the FeO_2 layers, it shows a large capacity decline due to the cationic disorder in the voltage region of 4.2–1.5 V.

Recently, Sakurai et al. [14] reported a new result that the corrugated $LiFeO_2$ material, which in synthesized by a H^+/Li^+ ion exchange method, could be easily obtained at low temperature when alcohol used as the reaction medium in the synthetic process. Furthermore, they succeeded in synthesizing another electrically active form of α-$LiFeO_2$ material, by reacting LiOH and α-FeOOH in 2-phenoxyethanol. It is known that lithium insertion/de-insertion occurs with difficulty into this material. Although this Li/α-$LiFeO_2$ cell delivered a small discharge capacity of

* Corresponding author. Fax: +81-45-508-7480.
E-mail address: satouy01@kanagawa-u.ac.jp (Y. Sato).

0378-7753/03/$ – see front matter © 2003 Elsevier Science B.V. All rights reserved.
doi:10.1016/S0378-7753(03)00152-6

50 mAh/g after 50 cycles, it is a fairly good cycling result, considering the electrochemical characteristics of the α-$LiFeO_2$ compound [15].

From a review of previous studies, we found that most $LiFeO_2$ materials were obtained using a complex reaction mechanism (e.g. ion exchange reaction, hydrothermal method). It needed a long reaction time or other reaction steps against the conventional solid-state method. Therefore, we report here a new and easy synthetic method of orthorhombic $LiFeO_2$ with good battery performance using a conventional solid-state reaction at low temperature and present the unique structural change of the orthorhombic $LiFeO_2$ material during cycling.

2. Experimental

$LiFeO_2$ was synthesized using $LiOH{\cdot}H_2O$ (Kishida Chemical, Japan) and γ-FeOOH (High Purity Chemicals, Japan) by a conventional solid-state method. A stoichiometric amount of each material was ground and calcined at 150 °C for 15 h in an argon atmosphere in a box furnace. The contents of Li and Fe in the resulting material were analyzed with atomic absorption spectroscopy (AAS, AA-6200, Shimadzu, Japan) by dissolving the powder in dilute nitric acid.

Powder X-ray diffraction (XRD, Rint 1000, Rigaku, Japan) using Cu Kα radiation was employed to identify the crystalline phase of the synthesized material. To investigate the structural differences of the positive electrode before and after capacity loss, each tested cell was left in a glove box for 2 days to reach equilibrium after cycling. The electrodes after cycling were washed with DMC solution to remove $LiPF_6$ salt. The particle morphology of $LiFeO_2$ material was observed using a transmission electron microscope (TEM, JEM 2010, JEOL, Japan) equipped with an energy-dispersive X-ray spectrometer (EDS).

Electrochemical characterization was performed using a CR2032 coin-type cell. The cathode was fabricated with 20 mg of accurately weighed active material and 12 mg of conductive binder (8 mg of Teflonized acetylene black (TAB) and 4 mg of graphite). It was pressed onto a 200 mm^2 stainless steel mesh used as the current collector under a pressure of 300 kg/cm^2 and dried at 130 °C for 5 h in an oven. The test cell was made of a cathode and a lithium metal anode (Cyprus Foote Mineral Co.) separated by a porous polypropylene film (Celgard 3401). The electrolyte used was a mixture of 1 M $LiPF_6$-ethylene carbonate (EC)/dimethyl carbonate (DMC) (1:2, v/v, Ube Chemicals, Japan). The charge and discharge current density was 0.4 mA/cm^2 (or 0.1 mA/cm^2) with cut-off voltages of 1.5–4.5 V at room temperature.

A three-electrode glass cell was used for cyclic voltammetry measurements. The working electrode consisted of 3 mg of the active material and 2.2 mg of conducting binder (TAB), which was pressed onto stainless steel mesh. The counter and reference electrodes were prepared by pressing lithium foil onto stainless steel gauze. The CV measurement was performed with an Arbin Instruments, model MSTAT4 battery test system at 0.2 mV/s scan rate between the voltage limits of 1.5–4.5 V. All assembly of the cell was carried out in a dry box with argon gas.

3. Results and discussion

To synthesize orthorhombic $LiFeO_2$ (herein referred to as o-$LiFeO_2$) by a conventional solid-state reaction, two mixtures of the LiOH and γ-FeOOH starting materials were thoroughly ground for 20 min in a mortar. One was calcined in a ceramic boat without pressing; the other was pressed at a 300 kg/cm^2 pressure into a 20 mm diameter pellet to improve the reactivity between the particles of the precursor.

Fig. 1 shows X-ray diffraction patterns (XRD) of the raw γ-FeOOH and the two $LiFeO_2$ materials that were calcined at 150 °C for 15 h in an Ar atmosphere. The $LiFeO_2$ mixture without pressing (Fig. 1(b)) shows a very similar XRD pattern when compared to the γ-FeOOH. It seems to have failed to form an orthorhombic structure, although there are some differences with that of the original γ-FeOOH, which resulted from the reaction with lithium hydroxide at 80 °C. On the other hand, Fig. 1(c) displays a well-defined orthorhombic pattern in the XRD diagram. The characteristic indications of the o-$LiFeO_2$ material are the well-defined split between the (0 1 1) and (1 1 0) peaks and between the (0 1 2) and (2 0 0) peaks, although there is a small amount of β-$LiFe_5O_8$ impurities. We found that in this study, pelletizing played an important role in accelerating the slow reaction between the lithium hydroxide and γ-FeOOH particles because the rate of the surface reaction between the two starting materials occurs slowly at a low synthesis temperature.

Fig. 2 shows the transmission electron microscope bright field image and selected area electron diffraction (SAD)

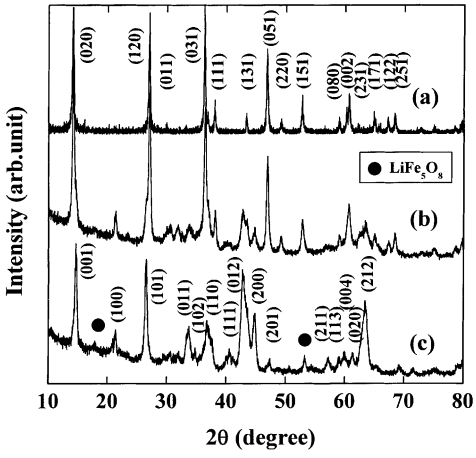

Fig. 1. X-ray diffraction patterns of: (a) raw γ-FeOOH; (b) $LiFeO_2$ without pressing; (c) $LiFeO_2$ with pressing.

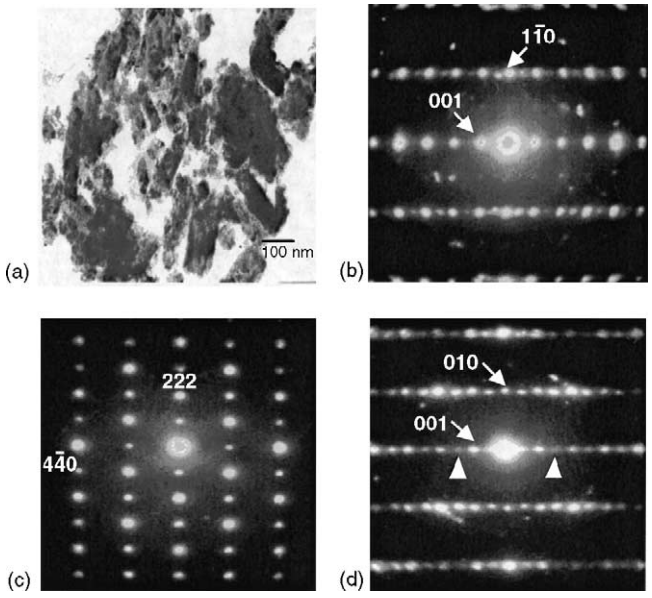

Fig. 2. TEM image and SAD patterns of resulting powder: (a) bright field image of orthorhombic $LiFeO_2$; (b) orthorhombic $LiFeO_2$ in [1 1 0] direction; (c) spinel β-$LiFe_5O_8$ in [1 1 2] direction; (d) defective $LiFeO_2$ in [1 0 0] direction.

patterns of the o-$LiFeO_2$ material. All the electron diffraction patterns were obtained from o-$LiFeO_2$ particles in this study. It shows that the $LiFeO_2$ sample consisted of 100–200 nm sized needle-type particles. It is composed of an orthorhombic phase ($a = 4.0$ Å, $b = 3.0$ Å, and $c = 6.1$ Å) with a small amount of β-$LiFe_5O_8$ ($a = 8.3$ Å) phase (Fig. 1(c)). Additionally, some of the orthorhombic phases (Fig. 2(d)) had different stacking sequencings in the c-direction, giving rise to a superlattice peak. The white arrows indicate the spots arising from the superlattice generated by the altered stacking sequence in the c-direction as shown above. We assume that the altered stacking sequence and higher spinel phase amount have combined to decrease the discharge capacity of the $LiFeO_2$ material. From the TEM analysis, it was found that the $LiFeO_2$ powder in this study was mixed with well-crystallized orthorhombic $LiFeO_2$, β-$LiFe_5O_8$, and defective $LiFeO_2$ phases.

Fig. 3 shows the charge/discharge curves for Li/1 M $LiPF_6$-EC/DMC/$LiFeO_2$ calcined at 150 °C for 15 h in an argon atmosphere. The test condition was a current density of 0.1 mA/cm^2 between 4.5 and 1.5 V (Fig. 4). The first charge of the Li/$LiFeO_2$ cell rapidly increased to 4.0 V and showed a plateau region between 4.2 and 4.3 V. The first discharge curve abruptly decreased below 3.5 V and displayed a voltage plateau in the 2.0–2.1 V region followed by two more small voltage steps. From the second cycle, the plateau region in the 2.0 V region was not detected and a slightly different cycle behavior was exhibited. This means that in the Li/$LiFeO_2$ cell there occurred a structural change during the first lithium insertion into the $Li_{1+x}FeO_2$ layers. As stated in previous reports, the Li/$LiFeO_2$ cell showed an abrupt capacity loss of about

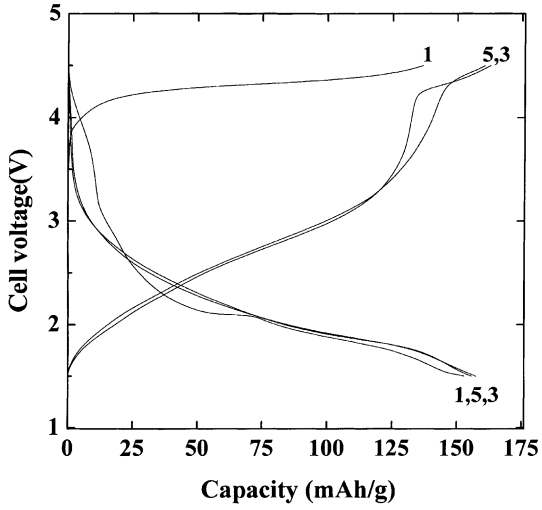

Fig. 3. The charge/discharge curves for the Li/1 M $LiPF_6$-EC/DMC/$LiFeO_2$ calcined at 150 °C for 15 h in argon. The test condition was a current density of 0.1 mA/cm^2 between 4.5 and 1.5 V at room temperature.

15–20% at a low current density (0.1 mA/cm^2) after the first cycle, which is due to a similar structure change as mentioned above. However, this Li/o-$LiFeO_2$ cell exhibited a very high initial capacity of about 152 mAh/g, which was one of the previously reported highest values, and had a slightly increased discharge capacity on the third cycle, although it exhibited a reduced discharge capacity in the second cycle. This point is one important characteristic of orthorhombic $LiFeO_2$ with nano-crystalline structure in this study. This $LiFeO_2$ compound was composed of lots of small nano-sized particles and these nano-particles improved the structural stability of $LiFeO_2$ powders, even though these had stress by the structural changes in the first cycle. Furthermore, we believe that large discharge capacity of the Li/$LiFeO_2$ cell in this study might result from the absence (or scarcity) of the inactive α-$LiFeO_2$ impurity in the $LiFeO_2$ structure.

To better understand the irreversible cycle behavior during the first discharge process, a cyclic voltammetry analysis was carried out at a sweep rate of 0.2 mV/s between the voltage limits of 1.5–4.5 V (Li/Li$^+$). The discharge process below the 3.5 V region consisted of four distinct peaks, which might be related to the structural transformation during the first cycling. This result agrees well with the charge/discharge curve of Li/$LiFeO_2$ cell as shown in Fig. 3. Almost all the peaks, especially the 1.76 V peak, abruptly decreased and maintained almost the same reduction shape after the second cycle. Based on this result, we assumed that the orthorhombic $LiFeO_2$ compound underwent a structural change during the first lithium insertion into the $Li_{1+x}FeO_2$ layers and maintained the changed structure after the second cycle.

In order to investigate the structure change observed with the Li/$LiFeO_2$ cell after the first cycling, ex situ XRD measurements were taken of four $LiFeO_2$ electrodes in

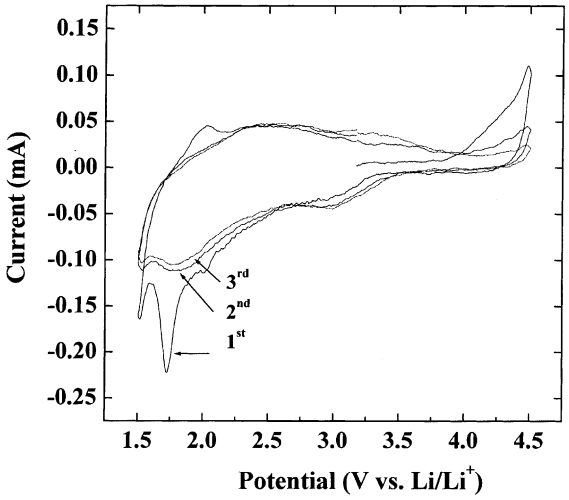

Fig. 4. Cyclic voltammogram of $LiFeO_2$ material. The scan rate was 0.2 mV/s between 4.5 and 1.5 V at 25 °C.

the discharged state after various cycles as shown in Fig. 5. The results of this ex situ XRD analysis show a remarkable change in the (0 0 1) peak at about $2\theta = 14.6°$, which is a characteristic peak of the orthorhombic structure in the XRD diagram. As the cycling proceeded, the intensity of the (0 0 1) peak gradually decreased. Moreover, the XRD pattern after 50 cycles was very similar to that of the spinel $LiFe_5O_8$ (α- or β-form). This means that the orthorhombic $LiFeO_2$ has a tendency to undergo a structural change during the cycle testing and ultimately reach the spinel phase after long-term cycling. Kanno and coworkers have already suggested that the conversion from the corrugated layer structure to an amorphous phase is due to the unstable $LiFe_2O_4$ spinel structure in the iron system. However, we have reported a new result here that the orthorhombic $LiFeO_2$ underwent a structural change to the spinel phase ($LiFe_5O_8$) during the charge/discharge process, which resulted in the capacity decline of the Li/$LiFeO_2$ system. A similar indication has also been reported in the orthorhombic Li/$LiMnO_2$

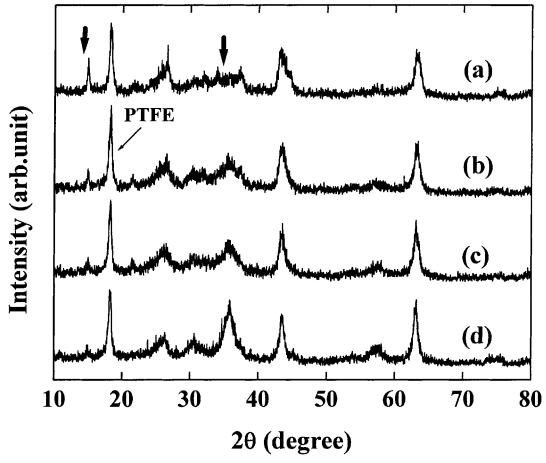

Fig. 5. Ex situ XRD patterns of $LiFeO_2$ electrodes in discharge state after: (a) third cycle; (b) 10th cycle; (c) 15th cycle; (d) 50th cycle.

system. Many research groups proposed that the capacity loss mechanism of the Li/$LiMnO_2$ cell is due to the conversion from the orthorhombic to spinel structure based on various analysis techniques [5,6,16,17]. Therefore, we suggest that the main capacity loss of the Li/$LiFeO_2$ cell is also based on the structure change from orthorhombic to the spinel phase during cycling. Furthermore, we are also studying ways to reduce the structural change in the first cycle [18] and increasing the low average working voltage of Li/$LiFeO_2$ cell, which is one serious handicap for practical utilization. A more detailed discussion about these points will be reported elsewhere.

4. Conclusion

A well-defined orthorhombic $LiFeO_2$ material has been synthesized at low temperature using a pressing process. It was composed of orthorhombic $LiFeO_2$, small amounts of the spinel $LiFe_5O_8$, and defective $LiFeO_2$ phases. The Li/$LiFeO_2$ cell showed not only a fairly high initial discharge capacity over 150 mAh/g, but also a good cycle retention rate at room temperature. We found that the orthorhombic $LiFeO_2$ underwent a structural change to the spinel phase during the charge/discharge process, which might be the main reason for the induced capacity loss during the long-term cycling.

Acknowledgements

The authors gratefully acknowledge the financial support to the High-Tech Research Center Project from the Ministry of Education, Culture, Sports, Science and Technology.

References

[1] K. Mizushima, P.C. Jones, P.J. Wiseman, J.B. Goodenough, Mater. Res. Bull. 15 (1980) 783.
[2] J.R. Dahn, U. Von Sacken, C.A. Michel, Solid State Ionics 44 (1990) 87.
[3] T. Ohzuku, A. Ueda, M. Nagayama, J. Electrochem. Soc. 140 (1993) 1862.
[4] H. Arai, S. Okada, Y. Sakurai, J. Yamaki, Solid State Ionics 95 (1997) 275.
[5] L. Croguennec, P. Deniard, R. Brec, A. Lecerf, J. Mater. Chem. 5 (1995) 1919.
[6] Y.I. Jang, B. Huang, H. Wang, D.R. Sadoway, Y.M. Chiang, J. Electrochem. Soc. 146 (1999) 3217.
[7] R. Kanno, T. Shirane, Y. Kawamoto, Y. Takeda, M. Takano, M. Ohashi, Y. Yamaguchi, J. Electrochem. Soc. 146 (1996) 2435.
[8] T. Shirane, R. Kanno, Y. Kawamoto, Y. Takeda, M. Takano, T. Kamiyama, F. Izumi, Solid State Ionics 79 (1995) 227.
[9] M. Tabuchi, K. Ado, H. Sakaebe, C. Masquelier, H. Kageyama, O. Nakamura, Solid State Ionics 79 (1995) 220.
[10] M. Tabuchi, C. Masquelier, T. Takeuchi, K. Ado, I. Matsubara, T. Shirane, R. Kanno, S. Tsutsui, S. Nasu, H. Sakaebe, O. Nakamura, Solid State Ionics 90 (1996) 129.

[11] K. Ado, M. Tabuchi, H. Kobayashi, H. Kageyama, O. Nakamura, Y. Inaba, R. Kanno, M. Takagi, Y. Takeda, J. Electrochem. Soc. 144 (1997) L177.
[12] M. Tabuchi, S. Tsutsui, C. Masquelier, R. Kanno, K. Ado, I. Matsubara, S. Nasu, H. Kageyama, J. Solid State Chem. 140 (1998) 159.
[13] M. Tabuchi, K. Ado, H. Kobayashi, I. Matsubara, H. Kageyama, M. Wakita, S. Tsutsui, S. Nasu, Y. Takeda, C. Masqulier, A. Hirano, R. Kanno, J. Solid State Chem. 141 (1998) 554.
[14] Y. Sakurai, H. Arai, S. Okada, J. Yamaki, J. Power Sources 68 (1997) 711.
[15] Y. Sakurai, H. Arai, J. Yamaki, Solid State Ionics. 113–115 (1998) 29.
[16] L. Croguennec, P. Deniard, R. Brec, J. Electrochem. Soc. 144 (1997) 3323.
[17] Y.S. Lee, M. Yoshio, Electrochem. Solid State Lett. 4 (10) (2001) A166.
[18] Y.S. Lee, Y.K. Sun, K. Kobayakawa, Y. Sato, Chem. Lett. (2002) 642.